Unsteady numerical analysis of heat transfer and phase change during crystal growth process

S. ZERMOUT[1], F. MOKHTARI[2], F.HADDAD[2], A.MERAH[2,3], I.LASLOUDJI[2]

[1]University Mouloud Mammeri of Tizi Ouzou, ALGERIA
[2]LTSE Laboratory, University of Science and TechnologyHouariBoumediene. BP 32 Elalia, BabEzzouar, Algiers, ALGERIA
[3]University M'hammed Bougara of Boumerdes UMBB, Boumerdes, ALGERIA
Faiza_mokhtari@yahoo.fr

Abstract: - Controlling the melt-crystal (m-c) interface during Kyropoulos crystal growth and understanding the origin of re-melting phenomenon are challenging tasks for sapphire crystal growers. In this paper, a transient model is used to investigate the evolution of the melt-crystal interface in Kyropoulos crystal growth of sapphire. Internal radiation in semi-transparent sapphire is modelled with the discrete ordinates model (DO) and the phase change with the enthalpy method. During crystallization, the maximum convexity of the m-c interface coincides with the development of an angle on the m-c interface near the free surface leading to the appearance of re-melting zone that affects the sapphire single crystal quality and reduces significantly the ingot diameter. This simulation also shows that the m-c interface shape and the crystal length obtained at different growth stages agree well with the experimentally grown crystals including re-melting zones phenomenon.
Keywords: heat transfer, crystal growth, Sapphire, unsteady simulation, re-melting phenomenon, mc interface.

1 Introduction

There is a growing interest on sapphire single crystals since they are widely used in a variety of modern high-tech applications as commercial optical systems, high power laser components and as excellent substrates for silicon-on-sapphire wafers. Czochralski (Cz) [1-3], heat exchanger method (HEM) [4-6], edge-defined film fed growth (EGF) [7] and Kyropoulos method [8.9] are among several growth techniques of sapphire crystals. The phenomenon known as "remelting-zones" is the main problem encountered during Kyropoulos process inducing defects that can degrade the crystal quality and affect their mechanical properties. Some authors have studied this phenomenon and proposed solutions to delay its onset. S.E.Demina et al. [9] have found a large vortex in almost entire melt and a secondary vortex of lower intensity near the free surface that changes the m-c interface shape and leads to re-melting-zone.

C. Chen et al. [10] have noted that a particular shape may delay the onset of re-melting phenomenon and reduces the convexity at the last stage of growth process. Internal radiation at different stages of Kyropoulos sapphire growth and their effect on the m-c interface and remelting-zone have been investigated by H.S.Fang et al [11]. They have concluded that both natural and thermocapillary convection in early growth stage influence the occurrence of re-melting zone.

Demina et al. [9] have shown that during the sapphire crystal stage growth, the maximum value of thermal stress is located along the crystallization front and close to the seed. W. J. Lee et al. [12] considered that a crucible with curved bottom reduces the convexity of the melt-crystal interface and the maximum velocity near the crystallization front than that of cylindrical crucible. Chun-Hung Chen et al. [13] have numerically simulated the thermal distribution and the von Mises stress in sapphire during the whole cooling process in a Kyropoulos furnace. They found that the highest stress appears in the near region of the seed crystal, the center and at the outer surface.

However, although there have been many studies on steady and quasi-steady simulations, as mentioned above, there has no report on transient computation on Kyropolous process and the origin of the re-melting zone occurrence is not well known. Hence, the main goal of this work is to have an insight into the time history of the m-c interface evolution in Ky process and the re-melting zone origins. Time-dependent finite volume method is used in computations, enthalpy porosity formulation for the phase change and discrete ordinates for radiations.

Results for growth front, crystal length and convexity during the whole growth process are presented. Melt convection and temperature field in melt and crystal are reported for the earlier growth stages. Comparison to previous experimental and numerical results is given when it is possible.

2 Numerical modelling

Schematic diagram of the whole Kyropoulos furnace is depicted in Fig. 1. The crucible and molten sapphire are heated through radiation, and cooled by the seed as well as support by conduction. This heat arises from three zones: upper, side and bottom heaters. Insulation shields are surrounding the crucible walls and heaters to avoid heat loss from the chamber furnace. In the liquid sapphire heat is transferred by convection and internal radiation.

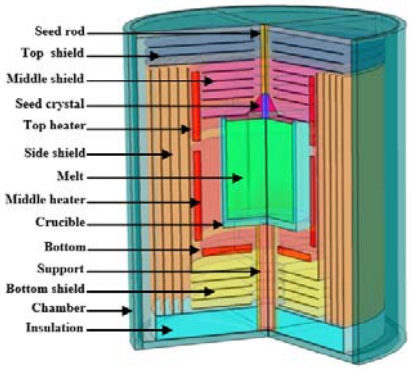

Fig. 1. Schematic diagram of Kyropoulos furnace

The melt sapphire is assumed to be laminar incompressible and Newtonian fluid satisfying the Boussinesq approximation.

The unsteady governing equations for the problem can be expressed in the following form:

$$\nabla.\vec{u} = 0 \quad (1)$$

$$\rho\frac{\partial\vec{u}}{\partial t} + \rho\vec{u}.\nabla\vec{u} = -\nabla p + \nabla.\left(\mu\left(\nabla\vec{u}\right)\right) + \rho\vec{g}\beta\left(T - T_m\right)/C_p - S_{\vec{u}} \quad (2)$$

$$\rho C_p\frac{\partial T}{\partial t} + \rho C_p\vec{u}.\nabla T = \nabla.\left(k\nabla T\right) + \nabla.q_{rad} - S_T \quad (3)$$

Where $\vec{u}$, T, P and t are velocity, temperature, pressure and time. ρ, μ, β, C_p, k and $\vec{g}$ represent density, dynamic viscosity, thermal expansion coefficient, specific heat, thermal conductivity and gravitational acceleration vector, respectively. $S_{\vec{u}}, S_T$ and $\nabla.\vec{q}_{rad}$ are source terms.

The model used for solving the phase change is based on the enthalpy formulation [14-16].

The growth interface is a porous region of a porosity equal to the liquid fraction fl. The relationship between the liquid fraction and temperature is defined as follows:

$$f_l = \begin{cases} 1, T \geq T_m & \text{melt} \\ 0, T < T_m & \text{crystal} \end{cases} \quad (4)$$

Where T_m is the melting temperature of sapphire.

The term source in the momentum equation is,

$$S_{\vec{u}} = A_{mush}\left(1 - f_l\right)\vec{u}$$

.

It serves to block the velocities in solid cells. The mushy zone constant Amush characterising the melt-crystal interface quantifies the loss of speed in the phase change zone. The enthalpy method [15,16] takes into account the latent heat of solidification L corresponding to the cell temperature in the following source term,

$$S_T = \rho.C_p.L\frac{df_l}{dt}$$

(5)

Choosing the right model of internal radiation in semi-transparent oxide crystals is of great importance for an accurate simulation of advancing m-c interface and the predictions of the temperature field.

In our work, the DO method is used for the internal radiation. Radiative heat transfer in the semi-transparent sapphire is calculated by the divergence of radiation flux defined by Eq. (6) in a particular direction $\vec{s}$:

$$\nabla.\left(I\left(\vec{r},\vec{s}\right)\vec{s}\right) + aI\left(\vec{r},\vec{s}\right) = an^2 I_b,$$

(6)

I is the radiation intensity at position $\vec{r}$ in direction $\vec{s}$, a is the absorption coefficient, n is the refractive index and I_b is the black body intensity given by Planck function. The 4π solid angle domain is divided into10x10 discrete, nonoverlapping solid angles and the partial differential equation for the radiative intensity in the discrete direction spanning the solid angle is obtained in Eq. (7). As a result, the radiative heat flux is as follows:

$$\vec{q}_{rad} = \sum_m \omega_m.\left(\vec{\Omega}_m.\vec{n}\right)I_m$$

(7)

where ω_m is the angular quadrature weigth which sums to the surface area of the unit sphere, I_m is the radiative intensity for the discrete direction $\vec{\Omega}_m$ and $\vec{n}$ is the unite normal vector. In this work, all walls are considered as opaque diffuse-gray boundaries.

Double precision solver of the finite volume method is used in simulation. The second order upwind discretization for convection, PISO algorithm for pressure-velocity coupling and the Pressure Staggering Option (PRESTO) scheme for pressure interpolation are employed.

3 Results and Discussion

The crystallisation front plays a great importance in the crystal quality. This is why we conducted transient simulations of the sapphire crystal growth process in a Kyropoulos furnace.

3.1 Melt-crystal interface morphology in time

Crystal-melt interface evolution versus time from the shouldering to the equal diameter until the ending growth stage is depicted in Fig. 2.

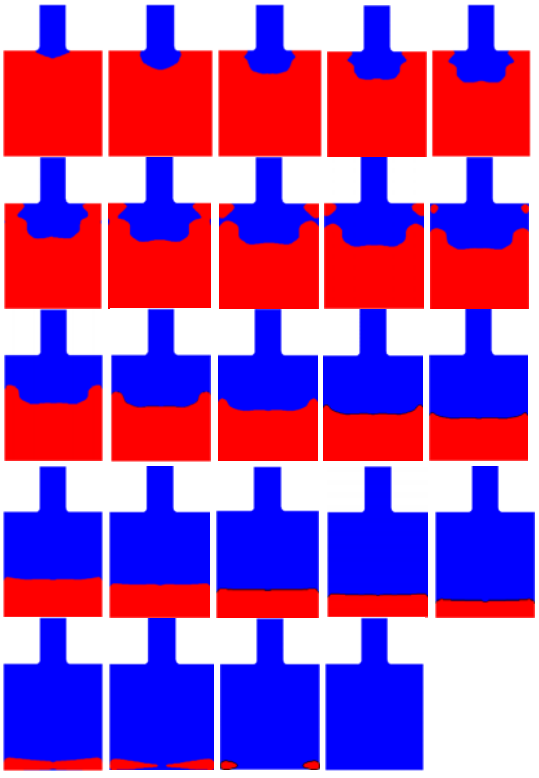

Fig. 2: Evolution of melt-crystal interface shape at different growth stages: Time interval between two successive cases is 2 hours.

The m-c interface morphology is conical downwards at the early growth stage (Fig.2a); the growth occurs mainly in the axial direction (z). This shape agrees well with experimental and numerical results [8,17,18].

Fig. 2b indicates that m-c interface shape becomes nearly hemispherical. At this stage, the growth arises in the radial and vertical directions. Thereafter, the interface loses its hemispherical shape and an obtuse angle (ɵ = 96º) directed towards the sidewall of the crucible appears, Fig. 2c. Reduction in melt volume and thus increase in crystal length characterise this growth stage.

The ɵ angle decreases over time to (90º, 81º, 74º), corresponding respectively to cases d-f. It orients its tip slightly toward the crucible wall up ɵ = 63º (Fig. 2g). At this growth stage, we notice that a small solid-spot appears on the sidewall of the crucible (Fig. 2f), which has no connection with the solid part. Gradually, this solid spot increases in size and meets ɵ angle (Figs. 2g, h). It appears then a liquid portion in form of a ring at the free surface near the sidewall. This sapphire liquid ring is isolated from the remaining melt inducing then the re-melting of the crystal portion in contact with the ring. Consequently, the irregular sapphire ingot shape resulting from remelting-zones appearance is probably caused by the unexpected formation of this molten sapphire ring at the free surface during the shouldering growth stage.

At intermediate stages, where the m-c interface advances downwards, this ring in turn decreases until it disappearance indicating the onset of the equal diameter stage (Figs. 2i-k). A wavy m-c interface shape results from the solidification of this ring. However, we observe in Figs. 2m-o that the m-c interface becomes almost flat with slight undulation close to the sidewall. Gradually, these undulations flatten throughout the bulk (Figs. 2p-t). At the ending growth stage (figs. 2u-x), the advancement m-c interface is faster at the central part than the side part, leading thus to the loss of the interface flatness. Fig. 2w shows that stagnation region appears in the crucible corner. A curved crucible bottom shape has been proposed to avoid the formation of this dead fluid region [12]. Stage x corresponds to the fully solidification of the sapphire melt.

The growth interface convexity is among the most important parameters affecting the crystal quality. Small convexity of the m-c interface is required to obtain good ingot quality. The convexity of the m-c interface defined by Chen et al [6] is expressed by:

$$C = \max Zh - \min Zh$$

Zh is the height of the m-c interface in the z direction.

Evolution of m-c interface convexity versus crystal length (H) is illustrated in Fig. 3a. We note that the convexity increases rapidly until a crystal length H = 186 mm and reaches its maximum value at point g, the stage just before the molten sapphire ring appearance.
Thereafter, the convexity decreases until the point p then remains almost uniform corresponding to the flatness of the growth interface during the equal-diameter stage. At this growth stage, the ingot part has a better quality than the shouldering stage [19].
At the end growth stage, a slight linear increase of the convexity is reported corresponding to the change from flat interface shape to slight conical (point, u). Afterwards, the convexity decreases faster while the crystal length remains fixed (u-x).

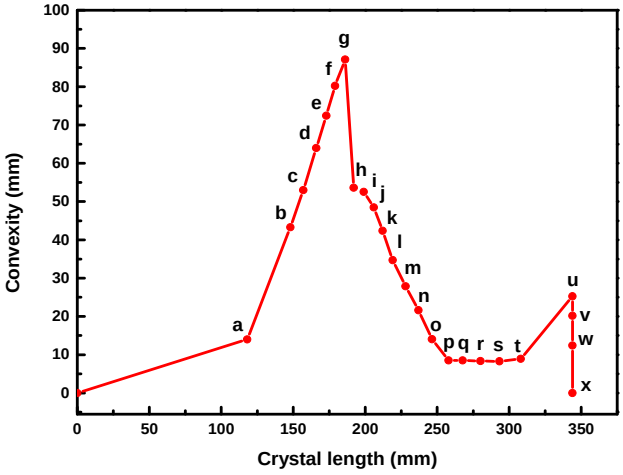

Fig. 3: a) m-c interface convexity evolution versus crystal length b) Crystal length evolution versus time at different growth stages

Crystal length evolution over time is presented in Fig. 3b. The growth process can be partitioned into three zones I, II and III following the different curve slopes.

The first growth stage (part I) corresponds to a fast increase of crystal length. At the atomic scale, such growth rate at the shouldering stage prevent the atoms to arrange themselves in a periodic array. This lack of a systematic atomic arrangement induces defects in the crystal [19]. At the equal diameter stage (part II), the crystal length increases linearly at a growth rate of about 4.19 mm/h. This small and uniform growth rate allows atoms self-organize following well-defined crystalline lattice resulting then in a good quality of this part. At the part III, a linear increase in length is reported before it approaches the crucible base.

3.2 Flow and temperature field

Isotherms and flow motion in the melt and temperature distribution in the sapphire crystal at the six earlier growth stages are depicted in Fig. 4.

The temperature evolution in the crystal indicates that heat is conducted from the melt to the crystallisation front by convection and internal radiation. Then transported from the hot m-c interface to the as-grown crystal by internal radiation and conduction, both of which are responsible for the quite convex isothermal lines in the crystal. However, the isothermal lines are distorted in the melt. This can be explained that the melt convection strongly affects the temperature field due to the high Prandtl number of the melt flow ($Pr = \mu.Cp/k = 40$).
The streamlines direction in the melt shows that under the buoyancy effect, the hot fluid particles move upward along the crucible sidewall, and then move radially along the melt free surface. Arriving at the growth interface, they become cold and heavy and under the gravity effect, they move downward along the centreline forming thus a vortex in the sapphire melt. Natural convection in the melt flow is mainly driven by the radial temperature difference. Grashof number ($Gr = \rho^2 g\beta R^3 \Delta T_{radial} / \mu^2$) represents the strength of natural convection in the molten sapphire, where R is the crucible radius. This number is approximately 4700. The low value of Gr indicates that the flow motion in the melt is laminar.

At the first growth stage (Fig. 4a), isotherms are concentrated near the m-c interface and have a conical shape. They appear sparse in the rest of the melt, which indicates that the temperature gradient is weak and more than half of the molten sapphire in the lower part of the crucible is almost at the same temperature.

This temperature distribution resulting from the transfer of heat by radiation and convection is responsible of the formation of an anticlockwise rotating vortex with a small intensity (Fig. 5a). Its center is located at the upper part of the melt and streamlines are closer together under the melt free surface.

At the second growth stage (Fig. 4b), isotherms become hemispherical near the m-c interface and slightly wavy in the rest of the melt and push towards the sidewall. This change in the temperature profile moves the vortex center to the molten sapphire center with a considerable increase in its intensity as shown in Fig. 5a.

From the third growth stage (Fig. 4c), sinuous isotherms induce an intensification and a moving downward of the vortex center. Then, streamlines become closer together near the bottom.

Gradually, as the crystallization front increases in size much more fluid becomes in contact with the m-c interface leading thus to the intensification of convection. Increasing the cold exchange surface, decreasing the melt free surface size and increasing the radial temperature gradient are among the origins of the intensification and the displacement of the vortex centre over time. Figs. 5a and 5b show that the vortex intensity and the center position stabilize for stages (c-f) where the melt free surface and the solidification front sizes remain almost the same.

Figs. 5c and 5d show that at the first growth stage, the axial temperature gradient is greater close to the m-c interface and decreases gradually as the growth process advances, while the radial temperature gradient decreases near the m-c interface and increases away from the m-c interface.

Let us now discuss the thermocapillary convection effect during the six earlier stages (Fig. 5). We observe that isotherms push to the sidewall inducing thus a decrease in the axial temperature gradient at the early growth stage of the process as shown in Fig.6a. This effect on the thermal gradient drops during the process (figs. 6b and 6c). Marangoni number,

$$Ma=-\left(d\gamma/dT\right)\left(1/\eta\alpha\right)R_2\left(T_{Free,max}-T_{Free,min}\right)$$

represents the strength of Marangoni convection caused by the surface tension gradients; it changes from 2500 to 1600.

Fig. 5b shows that Marangoni effect induces a remarkable increase of the vortex intensity at the beginning of the growth with a slight shift of its center (fig. 5a). This increase is estimated at 43% for the first stage and 5% for the second.

For the stages (c-f) in Fig. 6 corresponding to a small melt free surface size, the intensity of the buoyant vortex occupying practically all the melt and its location center remain unchanged. However, a secondary vortex of lower intensity induced by the surface tension gradients arises near the melt free surface. The formation of this second vortex is among the origins of the occurrence of remelting zones that significantly affect the ingot quality and size.

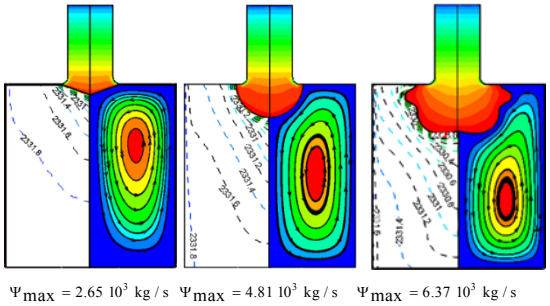

$\Psi_{max} = 2.65\ 10^3\ kg/s$ $\Psi_{max} = 4.81\ 10^3\ kg/s$ $\Psi_{max} = 6.37\ 10^3\ kg/s$

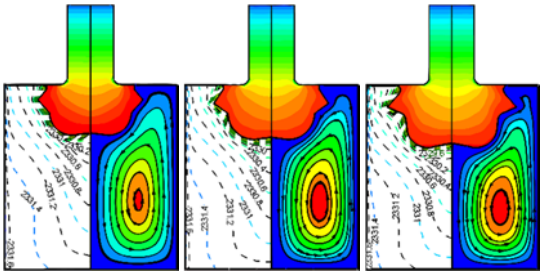

$\Psi_{max} = 6.22\ 10^3\ kg/s$ $\Psi_{max} = 6.38\ 10^3\ kg/s$ $\Psi_{max} = 6.3\ 10^3\ kg/s$

Fig. 4. Evolutions of temperature in the crystal, isotherms (left-hand side) and Streamlines (right-hand side) at the six earlier growth stages.

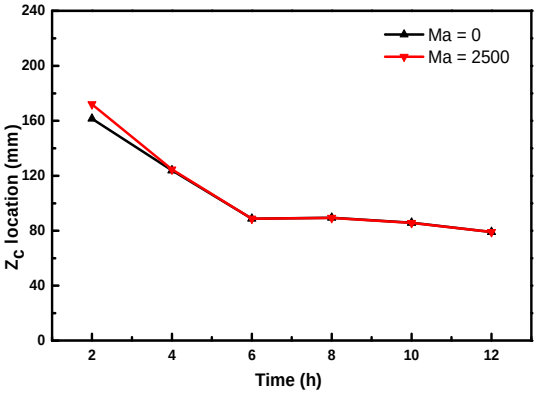

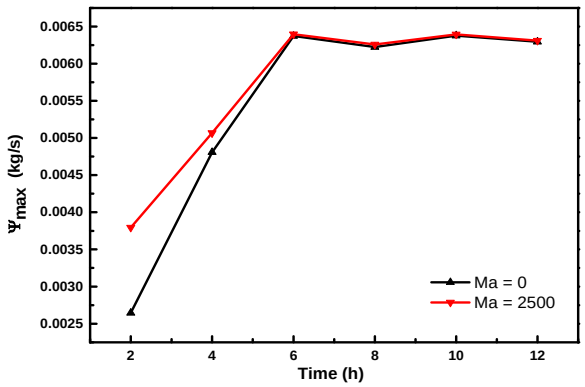

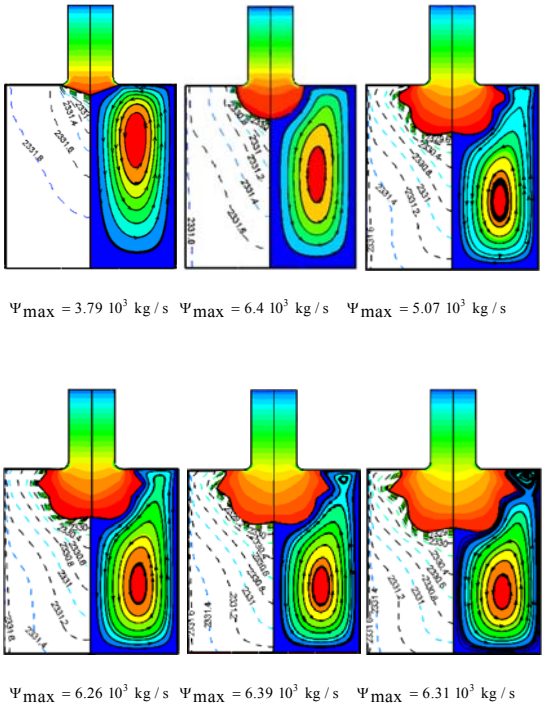

Fig. 6. Evolutions of isothermals (left-hand side) and Streamlines (right-hand side) at the earlier growth stages.

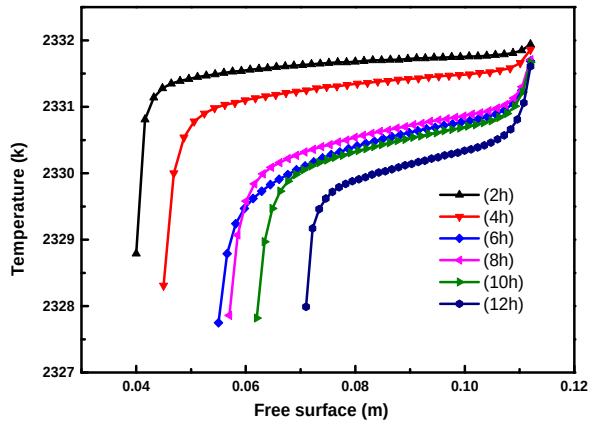

Figure. 5 : Effect of Marangoni convection

4. Conclusion

This investigation focuses on the analysis of the phase change phenomena during sapphire crystal growth process.

The m-c interface changes from conical to hemi-spherical morphology at the early growth stages then takes an undulate shape at the shoulder stage and gradually the m-c interface flattens at the equal diameter stage.

Growth rate corresponding to the equal diameter stage allows obtaining a good sapphire ingot quality comparing to the other stages. In addition, more than 45% of crystal was grown with average rate about 4.19 mm/h. = (Growth rate corresponding to the equal diameter stage allows obtaining large part and good sapphire quality comparing to the other part of ingot).

Convexity of the m-c interface shape reaches its maximum value when the hot liquid ring appeares

near the melt free surface and begins to decrease as it decreases. This convexity causes the development of a wavy interface shape on crystal surface periphery.

The temperature distribution predicted by this simulation shows that the isotherms accumulate in the crystal-solidified part. Isotherms in the melt are distorted by buoyancy and strongly affected by Marangoni convection.
Liquid sapphire ring appearance near the free surface at the shoulder stage increases the convexity of the m-c interface and causes the development of a wavy interface shape. When the remelting-zone occurs excessively, a significant portion of the ingot has a strong possibility of having microscopic and macroscopic defects that affect the crystal quality and subsequently translate into a loss of mass and energy during polishing.

Conical interface shape at the early growth stage, crystal length evolution over time and remelting occurrence show a sufficient agreement with available experimental works.

Finally, we believe that our work will be useful to clarify some points related to Kyropoulos crystal growth.

References

[1] H. S. Fang, J. Tian, S. Wang, Y. Long, M. J. Zhang and C. J. Zhao, Cryst. Res. Technol. 45, 371–379 (2010).
[2] H. S. Fang, J. Tian, S. Wang, Y. Long, M. J. Zhang and C. J. Zhao, Cryst. Res. Technol 49, 323–330 (2014).
[3] H. Li, E.A. Ghezal, A. Nehari, G. Alombert-Goget, A. Brenier, K. Lebbou, J. Optical Materials 35, 1071–1076 (2013).
[4] Chung-Wei Lu and Pei-Hung Chi, Cryst. Res. Technol. 42, Nº. 12, 1259 – 1265 (2007).
[7] O. Bunoiu, I. Nicoara, T. Duffar, J. Optoelectron. Adv. Mater. 7 (2) 615 (2005).
[8] S.E. Demina, E.N. Bystrova, M.A. Lukanina, V.M. Mamedov, V.S. Yuferez, E.V. Eskov, M.V. Nikolenko, V.S. Postolov, V.V. Kalaev, Opt. Mater. 30, 62-65 (2007).
[9] L. Zhang, H. Zuo, F. Cao, D. Xing, J. Sun Xiaohong Wang, and J. Han, Cryst. Res. Technol. 47, 175 – 182 (2012).
[10] C. Chen, H.J.Chen, W.B.Yan, C.H.Min, H.Q.Yu, Y.M.Wang, P.Cheng, C.C.Liu, J. Cryst. Growth 388, 29–34 (2014).
[11] H. S. Fang, S. Wang, Z. L. Jin, J. Tian, and J. F. Xu, Cryst. Res. Technol. 48, Nº. 9, 649–657 (2013).
[12] W.J. Lee, Y.C. Lee, H.H. Jo, Y.H. Park, J. Cryst. Growth 324, 248–254 (2011).
[13] H.S. Fang, Z.L. Jin, M.J. Zhang, Z. Zhang, C.J. Zhao, Int. J. Heat Mass Transfer 67, 967–973 (2013).
[14] V.R. VOLLER, Journal of Numerical Analysis, Vol 5, 201–214 (1985).
[15] V.R. Voller, C.Prakash, Int. J. Heat Mass Transfer. Vol.30 Nº 8, 1709-1719 (1987).
[16] A.D. Brent, V.R.Voller, K.J.Reid, Numerical Heat Transfer. Vol.13, 297-318 (1988).
[17] C.H Chen, J.ChenChen, C.WeiLu, C.MingLiu, J. Cryst Growth.352, 9–15 (2012).
[18] G. Alombert-Goget, K. Lebbou, N.Barthalay, H.Legal, G.Cheriaux, Opt Mater. 36, 2004–2006 (2014).
[19] Weichao Chen, Huili Tang, Jingya Wang, Qingxi Yuan, Dapeng Jiang, Xiaobo Qian, and Jun Xu, Cryst. Res. Technol. 49, Nº. 7, 507–513 (2014).